

1 ResORR: A Globally Scalable and Satellite
2 Data-driven Algorithm for River Flow
3 Regulation due to Reservoir Operations

4 Pritam Das¹, Faisal Hossain^{1*}, Sanchit Minocha¹, Sarath Suresh¹, George K.
5 Darkwah¹, Hyongki Lee², Konstantinos Andreadis³, Miguel Laverde-Barajas⁴ and
6 Perry Oddo⁵

7 ¹Department of Civil and Environmental Engineering, University of Washington, Seattle, WA, USA

8 ²Department of Civil and Environmental Engineering, University of Houston, Houston, TX, USA

9 ³Department of Civil and Environmental Engineering, University of Massachusetts, Amherst, MA, USA

10 ⁴Asian Disaster Preparedness Center, Bangkok, 10400, Thailand

11 ⁵Science Systems and Applications, Inc., Lanham, MD, USA

12

13 **Abstract:** We propose a globally scalable algorithm, ResORR (Reservoir Operations driven
14 River Regulation), to predict regulated river flow and tested it over the heavily regulated basin of
15 the Cumberland River in the US. ResORR was found able to model regulated river flow due to
16 upstream reservoir operations of the Cumberland River. Over a mountainous basin dominated by
17 high rainfall, ResORR was effective in capturing extreme flooding modified by upstream
18 hydropower dam operations. On average, ResORR improved regulation river flow simulation by
19 more than 50% across all performance metrics when compared to a hydrologic model without a
20 regulation module. ResORR is a timely software algorithm for understanding human regulation of
21 surface water as satellite-estimated reservoir state is expected to improve globally with the recently
22 launched Surface Water and Ocean Topography (SWOT) mission.

23

24 **Keywords:** River Regulation, Reservoir Operations, Hydrological Modeling, Satellite Remote
25 Sensing

26

27 **Highlights:**

- 28 • A globally scalable algorithm, called ResORR, to predict regulated flow from naturalized
29 flow and upstream reservoir storage is proposed.
- 30 • ResORR requires globally available satellite-based reservoir storage and satellite-forced
31 hydrologic model.
- 32 • ResORR was tested on the heavily regulated river basin of the Cumberland river in
33 Tennessee, USA.
- 34 • On average, ResORR improved regulation river flow simulation by more than 50% across
35 all performance metrics when compared to a hydrologic model without a regulation
36 module.
- 37 • ResORR is a timely software algorithm that can be further improved of its skill with
38 reservoir storage data from the Surface Water and Ocean Topography (SWOT) mission.

39
40

41 **Data and Software Availability:** The model code developed during this study is available on
42 GitHub (<https://github.com/UW-SASWE/ResORR>) under the MIT license. Documentation on
43 ResORR is available at - <https://resorr.readthedocs.io/en/latest/>? The github repository was created
44 by first author Pritam Das (pdas47@uw.edu). Author's experimental CPU environment used
45 Linux Ubuntu OS, Intel Xeon Scalable Gold 6242 at 2.8GHz (16-Core), 192GB RAM.

46

47 1. Introduction

48 Rivers have provided humans with food, water and energy security since human
49 civilization first started to take shape in ancient valleys of Tigris-Euphrates, Indus and Nile rivers.
50 This has only been made possible by means of control structures such as dams and reservoirs,
51 which allow storage and release of water from the river according to human needs. Usually, water
52 from the river is stored in reservoirs when the river naturally has higher flows, resulting in a net
53 reduction in the downstream flow of the river. This storage is driven by human needs such as flood
54 control or to meet future freshwater demand when natural availability may be insufficient. The
55 converse happens during naturally occurring periods of low flows, when release of water from
56 reservoirs artificially increases the downstream flow rate during the dry season to meet demand
57 for water. This regulation of surface water, in the form of alteration of the streamflow from its
58 natural pattern of discharge under pristine conditions, can be termed as river regulation.

59 River regulation can change how the basin responds to a hydro-meteorological event in the
60 form of precipitation or snowmelt, affecting its natural variability and streamflow timing. For
61 instance, Wisser and Fekete (2009) found that the average residence time has increased by 42 days
62 globally over the past century due to construction of reservoirs. Such disruption and alteration of
63 natural conditions is even more profound at a regional scale, for instance, Bonnema and Hossain,
64 (2017) note about 11-30% streamflow alteration in the Mekong basin, with the residence time of
65 reservoirs varying from 0.09 to 4.04 years. Vu et al., (2021) estimate that reservoirs in the Mekong
66 hold 50% of its dry season flow and 83% of its wet season flow. As a result, the high flows of the
67 Mekong-river have reduced by 31%, while the low-flows have increased by 35%.

68 River regulation can also have serious ecological repercussions. For instance, the unique
69 annual flow reversal of the Tonle Sap River (TSR) leading to filling up the Tonle Sap Lake (TSL)
70 during the wet season and draining it during dry season may cease to exist if the flood pulse of the
71 Mekong River dampens by 50% and is delayed by a month (Pokhrel et al., 2018). The absence of
72 this unique flow reversal may have a negative impact on aquatic biodiversity, particularly for
73 fisheries and paddy planting (Marcaida et al., 2021). Similarly, in European rivers, high-flows
74 appear to be down by 10% while low-flows are up by 8% (Biemans et al., 2011). Negative
75 consequences are not limited to only ecological aspects but can also influence the regional demand-
76 and-supply of resources, with the potential to escalate pre-existing water conflicts. The
77 construction and filling up of the Grand Ethiopian Renaissance Dam (GERD) on the Nile River
78 has been a source of contention between Ethiopia and the other riparian countries – Egypt and
79 Sudan. Eldardiry and Hossain, (2021) estimate that if unprepared, the High Aswan Dam (HAD) –
80 a dam of existential importance to Egypt for its water-food-energy security – may take anywhere
81 from 2 years to 7 years to fully recover following the filling-up of the GERD. Although, they also
82 optimistically estimate that with cooperation and planning between the riparian countries, the
83 recovery period can be limited to immediate 2 years.

84 Apart from the direct alteration of streamflow timing of rivers, regulation due to dam and
85 reservoir operations can have an indirect effect on other components of the eco-system. For
86 instance, river regulation disturbs the natural sediment flow, resulting in a net reduction in
87 sediment deposition along shorelines of rivers, estuaries and oceans (Dunn et al., 2019; Li et al.,
88 2021). River water temperature anomalies owing to thermal stratification in reservoirs have also
89 been widely recognized (Ahmad et al., 2021; Cheng et al., 2020). Considering the sensitivity of
90 aquatic life to the water temperature changes (Caissie, 2006), river regulation can negatively affect

91 the environmental suitability for aquatic organisms (Cheng et al., 2022). Such negative
92 environmental consequences are a direct result of human decisions – which many consider
93 necessary to support the demands of a rapidly growing population. A better understanding of
94 human regulation of river flow, exacerbated by a changing climate and increasing freshwater
95 demand, is urgently required to ensure a sustainable future.

96 The coupled nature of human-water resources has led to developments in explicitly
97 modeling reservoir operations in Large-Scale Hydrological Models (LHMs) and Global
98 Circulation Models (GCMs) (Hanasaki et al., 2018; Wada et al., 2017). Existing methods to
99 represent human activities in hydrological models rely on modeling the optimal reservoir release
100 based on operating parameters such as the design role of the reservoir (Hanasaki et al., 2006), land-
101 water management schemes, downstream demand for water and energy (Alcamo et al., 2003;
102 Biemans et al., 2011; Haddeland et al., 2006; Vanderkelen et al., 2022). Many of these human
103 activities are often assumed or ‘parameterized’ due to lack of sufficient observational data on
104 reservoir operations. Using such a parameterized approach, Zhou et al. (2016) found that in highly
105 regulated basins, such as the Yellow and the Yangtze rivers, the seasonal reservoir storage
106 variations can contribute up to 72% of the variability of the basin’s total storage. While such key
107 insights can be obtained using generic schemes of reservoir operations, the underlying assumption
108 of optimal reservoir operations may not always hold true. Stakeholders and reservoir managers
109 must often deviate from optimal operating conditions based on a variety of reasons, such as
110 adapting to regional water and energy demands, new hydro-political reality, environmental
111 regulations, and changing weather and climate patterns that result in river flow to exceed the
112 bounds of pre-dam historical flow records.

113 In the past, modeling human decisions of reservoir operations using parameterizations or
114 criteria-based assumptions has been the primary way for characterizing river-regulation due to a
115 lack of publicly available observations on dam operations. However, to better understand river
116 regulation, which is representative of the intricacies of operation of individual reservoirs, we need
117 to characterize and quantify river regulation grounded in observations of reservoir operations
118 (Biswas et al., 2021; Das et al., 2022; Zhou et al., 2016). Earth observing satellites, with their
119 vantage of space and a multi-decadal record of observations on reservoir operations now provide
120 an opportunity to fill this data availability gap by inferring reservoir operations from space
121 (Bonnema & Hossain, 2017).

122 Studies have used satellite remote sensing-based reservoir operations monitoring
123 techniques to model the resulting regulation of streamflow. Reservoir releases are obtained by
124 typically assuming water mass balance at the reservoirs, by modeling the inflow and storage
125 change of the reservoirs. For instance, Yoon & Beighley, (2015) and Yoon et al., (2016) model
126 the inflow at reservoirs in the Cumberland basin due to surface runoff and upstream releases using
127 the Hillslope River Routing (HRR) model. The storage change is estimated using historical record
128 of reservoir operations by Yoon & Beighley, (2015) and by simulating SWOT-like storage change
129 estimates by Yoon et al., (2016). The performance of the simulated discharges in both cases
130 improves with the inclusion of reservoirs. Han et al., (2020) also take the approach of simulating
131 reservoir operations by deriving the operating curve of reservoirs using satellite observations.
132 Reservoir releases from upstream reservoirs were added to the inflow of downstream reservoirs in
133 a cascade reservoir system in the Mekong River basin. However, in this case the inclusion of
134 upstream releases did not improve the performance of regulated streamflow estimates drastically.
135 Dong et al., (2023) use historical satellite observations of reservoir water level to calibrate

136 parameters of a reservoir operation scheme. The reservoir releases are routed downstream using
137 the Coupled Land Surface and Hydrologic Model System (CLHMS). All the existing studies rely
138 on specific hydrological routing models to route the runoff and releases downstream. There doesn't
139 exist a method to leverage existing hydrological model setups, that are usually calibrated using
140 data that is only accessible to local stakeholders. Furthermore, the availability of high frequency
141 satellite observations near-real time provides an opportunity to move away from parameterization
142 and simulation driven estimation of reservoir operations to a direct observation-based approach
143 for modeling reservoir releases. Rather than relying on parameterized or criteria-based
144 assumptions of reservoir operations, we can now use actual observation-based reservoir operations
145 to quantify the regulation of flow in physical models. Because satellite observations today can
146 track the dynamic state of reservoirs comprising surface area, water surface elevation,
147 evapotranspiration losses, storage change and even outflow (Cooley et al., 2021; Hossain et al.,
148 2017; Lee et al., 2010; Okeowo et al., 2017; Zhao et al., 2022), there is now a stronger argument
149 to move away from assumptions and parameterizations in representing human flow regulation in
150 physical hydrologic models.

151 Satellites such as the Landsat, Sentinel, and Jason series have been extensively monitoring
152 hydrologically relevant aspects of the Earth's surface, such as surface reflectance and elevation, at
153 the global scale. For instance, Gao et al., (2012) were able to recreate storage variations of large
154 reservoirs using observations from the Moderate Resolution Imaging Spectroradiometer (MODIS)
155 satellite platform. Cooley et al., (2021) used NASA's ICESat-2 satellite observations of water level
156 height to estimate that about 3/5th of the Earth's surface water storage variability takes place due
157 to reservoirs. Moreover, the recently launched terrestrial hydrology-focused Surface Water and
158 Ocean Topography (SWOT) satellite is now expected to improve the monitoring of surface water
159 resources at an unprecedented scale and accuracy (Biancamaria et al., 2016). Together, these
160 Earth-observing satellites provide an opportunity to independently track various aspects of the
161 hydrological cycle, including reservoir operations (Bonnema & Hossain, 2017; Hossain et al.,
162 2017). Using multi-sensor satellite data on surface water, we can now build comprehensive,
163 distributed, and scalable modeling platforms to simulate reservoir-river systems. The Reservoir
164 Assessment Tool (RAT) is one such modeling platform that can estimate reservoir fluxes,
165 comprising inflow to the reservoir, storage change, evaporative losses and outflow, solely using
166 satellite data and hydrological modeling (Biswas et al., 2021; Das et al., 2022). More recent
167 developments have made it easier to monitor reservoirs using RAT, further democratizing the
168 availability of surface water data at the granular level for regulated river systems (Minocha et al.,
169 2023). This has allowed for both global and regional scale studies of the anthropogenic impact on
170 terrestrial water storage (Biswas & Hossain, 2022) and floods (Suresh et al., 2024), especially in
171 the regions of the world that lack a robust data collection and sharing infrastructure.

172 Considering the importance and urgency of an observations-driven understanding of river
173 regulation, there is now a need to develop methods to quantify river regulation due to reservoir
174 operations that can be scaled globally based on publicly and globally available satellite
175 observables. The wide availability of satellite-based reservoir operations data will only keep
176 increasing with the recent launch of the SWOT mission that is optimized for surface water tracking,
177 particularly for lakes and reservoirs. Here, the multi-satellite observations used by RAT to estimate
178 storage change (Das et al., 2022) can be directly used as observations to quantify river regulation,
179 obviating the need to separately model reservoir operations based on parameterizations or
180 operating assumptions, which can be both difficult and unrepresentative of actual reservoir
181 operations. Given the availability of multi-decadal satellite observations of surface water that are

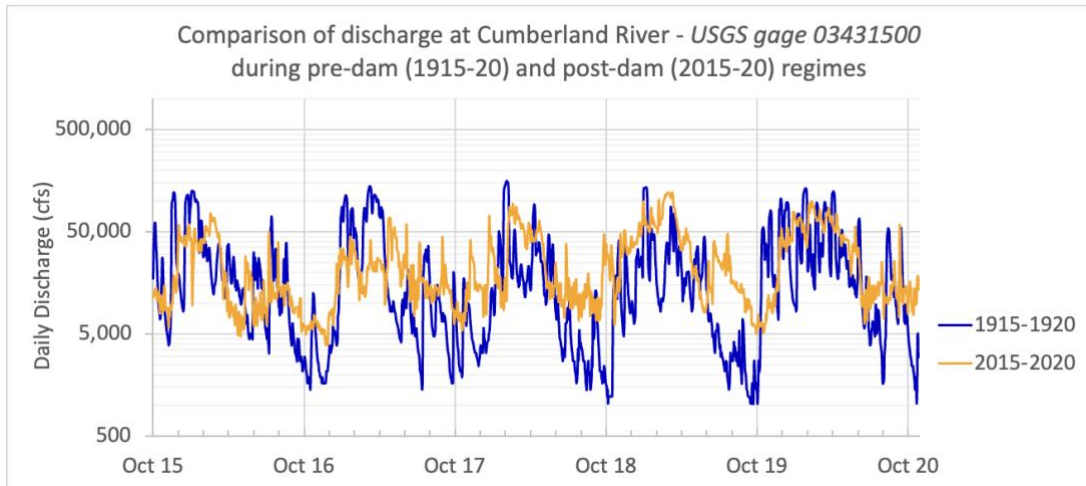
182 now made widely accessible due to advancements in information technology, we are now uniquely
183 positioned to predict regulated flow at a level of granularity that was not possible before.
184 Estimation of river regulation grounded in observational data inherently represents the actual or
185 likely decisions made by reservoir operators. The primary research question that this paper
186 addresses is – *How can river regulation due to operation of reservoirs be formulated in a globally*
187 *scalable format using primarily satellite observations?* The objectives of the paper are as follows:

- 188 1. To develop a globally scalable river-regulation algorithm based on satellite observables
189 or satellite derived reservoir data for predicting the human regulation of surface water.
- 190 2. To investigate incorporation of the river-regulation algorithm in the RAT modeling
191 platform for regulated rivers, and quantify its skill in capturing river flow regulation at
192 a basin scale.

193 2. Study area and Data

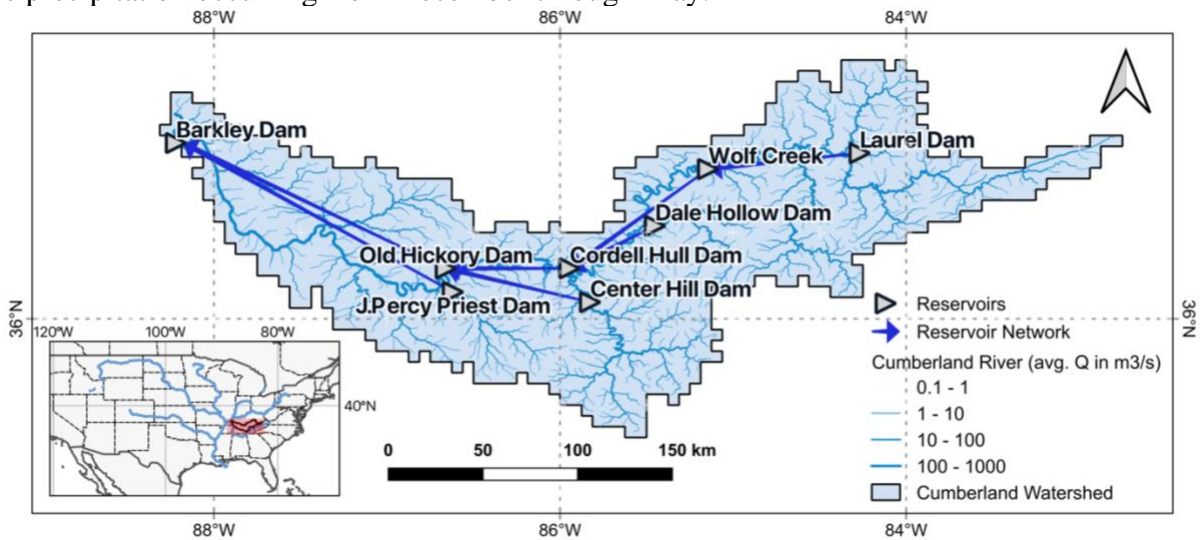
194 2.1. The Cumberland River in Tennessee, US

195 The Cumberland River is highly regulated by a system of 10 major dams and reservoirs
196 with varying primary use cases, making it one of the most heavily regulated basins. The United
197 States Army Corps of Engineers (USACE) Nashville District, own and operate 10 such multi-
198 purpose dam/reservoir projects on the Cumberland River, with the first dams being built in 1950s.
199 These dams are used for hydropower generation, flood control, recreation, commercial navigation,
200 public water supply, and fisheries and wildlife management – bringing in immense economic
201 benefits to the region (Robinson, 2019). Figure 1 compares the daily discharge in the Cumberland
202 River for two time-periods corresponding to unregulated conditions (1916-1920) and regulated
203 conditions (2016-2020). The effect of regulation can be clearly seen in the figure, in the form of
204 reduced range and variability in the discharge hydrograph. Studies suggest that such regulation has
205 caused a sharp decline in the population and species variety of Mussels in the basin, which were
206 plentiful when the river was unregulated (Neel & Allen, 1964; Tippit et al., 1995; Wilson & Clark,
207 1914). In addition to the highly regulated status of the basin, the availability of long periods of in-
208 situ observational data from the operating agencies makes this basin an ideal test bed for
209 investigating anthropogenic river regulation (Bonnet et al., 2015).



210
 211 Figure 1: Comparison of 5 years of daily discharge during (a) unregulated conditions, prior to
 212 construction and operation of major dams (1916-1920), and (b) regulated conditions, as observed
 213 in the Cumberland River near Nashville, TN. The flow rate in a regulated regime has a markedly
 214 attenuated peak-trough range – with low flows rarely dropping below 5000 cfs as compared to
 215 the unregulated regime when flow rates naturally used to drop to 1000 cfs. Source: United States
 216 Geological Survey (USGS).

217 Originating in the Appalachian Mountains, the Cumberland River flows westwards
 218 through the states of Kentucky and Tennessee in the United States, draining a region of about
 219 18,000 sq. miles (~45,000 sq. km), before merging into the Ohio River. Ten dams – Martins Fork,
 220 Laurel, Wolf Creek, Dale Hollow, Cordell Hull, Center Hill, Old Hickory, J. Percy Priest,
 221 Cheatham, and Barkley dams – are operated by USACE, with some additional dams operated by
 222 the Tennessee Valley Authority (TVA) (Robinson, 2019). Limited by the availability of in-situ
 223 reservoir operations data, 8 of the USACE owned dams were included in this study. Based on the
 224 conclusions of the study, the authors believe that the results are not affected by the exclusion of
 225 the 2 USACE dams owing to their relatively insignificant (Martin’s Fork dam) to no storage
 226 (Cheatham dam). The region generally has a temperate, warm, and humid climate, with most of
 227 the precipitation occurring from December through May.



228

229 Figure 2: Map of the Cumberland basin, showing locations of the reservoirs, the reservoir
230 network and the location of the Cumberland basin in the US.

231 2.2. In-situ and satellite observations of reservoir dynamics

232 To develop, test and validate the river-regulation algorithm, observed in-situ data
233 pertaining to reservoir operations – inflow, outflow, and storage – were used, which were obtained
234 from the ResOpsUS (Steyaert et al., 2022) dataset. This dataset is a compilation of in-situ reservoir
235 operations data for 679 major dams in the US, including 8 of the USACE dams in the Cumberland
236 basin and one dam operated by the TVA, until November 2019. Daily storage change was
237 calculated using the storage values in the dataset for all but 2 dams – Old Hickory and J. Percy
238 Priest – which had missing storage data from July 2015 onwards. The storage change for these
239 reservoirs were obtained by subtracting the reported Outflow from the Inflow ($\Delta S = I - O$).
240 Readers are referred to section 7.2 for more discussion on this data preparation step. The in-situ
241 data was also used to force the river-regulation model in certain experiments to compare the
242 sensitivity of the river-regulation model to the accuracy of input data – a detailed discussion is
243 provided in section 4.1. Additionally, the in-situ Area-Elevation Curve (AEC) of all the USACE
244 reservoirs were also obtained from the Access to Water Resources Data – Corps Water
245 Management System (CWMS) Data Dissemination tool (USACE, n.d.).

246 The latest version of Reservoir Assessment Tool (RAT 3.0) was used to obtain the storage
247 change and river flow under pristine (naturalized) conditions (assuming no upstream reservoirs).
248 Originally developed by Biswas et al., (2021), the RAT framework is designed to improve access
249 to information on reservoir dynamics, especially with recent developments leading to both a higher
250 performance and accessibility (Das et al., 2022; Minocha et al., 2023). Using the default
251 hydrological model of RAT, Variable Infiltration Capacity (VIC) (Liang et al., 1994), rainfall-
252 runoff modeling was performed at a 0.0625° spatial resolution. The inflow to each reservoir’s
253 location under natural conditions was estimated using the VIC-Routing model (Lohmann et al.,
254 1998), which uses the linearized Saint-Venant equation to route streamflow within the watershed.
255 The default VIC parameters, and sources of temperature and wind data used in RAT 3.0 were used
256 to force the hydrological model. The precipitation was obtained from the ERA-5 reanalysis dataset
257 (Hersbach et al., 2020). It must be noted here that the VIC-based reservoir inflow in RAT 3.0 does
258 not take upstream reservoir operations into account, and hence the need to develop a model that
259 can supplement the RAT framework by taking upstream regulation into consideration. A detailed
260 discussion on how the hydrological model’s estimated inflow in pristine conditions is used in the
261 river regulation model can be found in section 3.1. Since the in-situ AEC of the TVA-owned
262 reservoir was not available, the default AEC option in RAT 3.0 was applied based on the Shuttle
263 Radar Topography Mission Digital Elevation Model (SRTM DEM) (Earth Resources Observation
264 And Science (EROS) Center, 2017).

265 3. Methods

266 3.1. Reservoir Operations driven River Regulation (ResORR) – 267 Conceptual algorithm

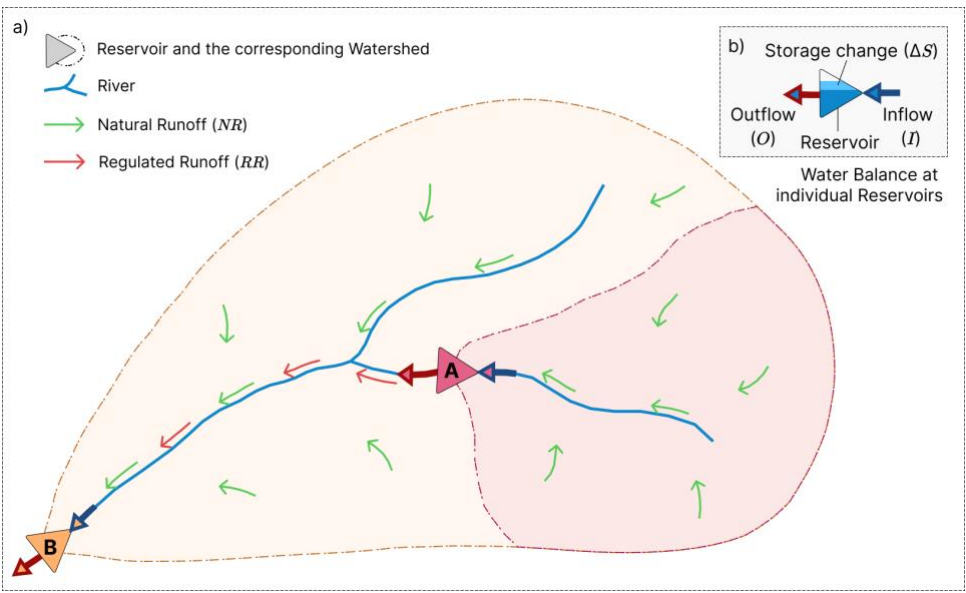
268 The core assumption of the ResORR algorithm is that the volume of water entering the
269 reservoir, Inflow (I), is composed of two components – natural and regulated. The Natural Runoff

270 (NR) is defined as the component of surface runoff that flows naturally into the reservoir without
 271 passing through any upstream reservoirs. Similarly, the Regulated Runoff (RR) is the component
 272 of surface runoff that first gets intercepted by an upstream reservoir before being released based
 273 on the reservoir's operations policy. The partitioning of the inflow to a reservoir is defined by the
 274 following equation,

$$I = NR + RR \tag{1}$$

275 Essentially, the problem of estimating the inflow at any reservoir is decomposed into the
 276 two parts of estimating the natural and regulated components of the incoming streamflow. A
 277 detailed discussion on estimating these sub-components of inflow is provided later in the section.
 278 The estimated inflow to a reservoir in this scheme will, hence, be affected by regulation due to
 279 upstream reservoir operations.

280 For example, consider the example of a two-reservoir system (A and B), where reservoir
 281 B is downstream of reservoir A, depicted in the schematic in Figure 3(a). In this scenario, the
 282 inflow at reservoir B would have contributions from the outflow of the upstream reservoir A in the
 283 form of RR (i.e., $RR \neq 0$), in addition to the NR. On the other hand, since reservoir A has no
 284 upstream reservoirs, the inflow to the reservoir would be fully natural, i.e., $RR = 0$ and $I = NR$.



285 Figure 3: Conceptual schematic of the ResORR model. Panel (a) depicts the flow of surface runoff
 286 and streamflow, along with the contribution of the natural (green arrows) and regulated (red arrows
 287 along the stream) components, referred to in this paper as Natural Runoff (NR) and Regulated
 288 Runoff (RR) to the Inflow ($I = NR + RR$) to a reservoir. Panel (b) describes the components of
 289 the water balance equation ($O = I - \Delta S$) used at the reservoir to obtain the outflow from the
 290 reservoir, which is treated as the regulated component of the downstream streamflow.
 291

292 As discussed above, the RR is defined as the component of inflow to a reservoir due to
 293 upstream reservoir releases. It is estimated as the sum of all Outflow (O) of the upstream reservoirs.

$$RR_i = \sum_j^N O_j \tag{2}$$

294 Where RR_i is the incoming Regulated Runoff to reservoir i ; O_j is the Outflow from the j^{th}
295 upstream reservoir; N is the total number of upstream dams for reservoir i .

296 The NR is defined as the volume of water inflow to the reservoir due to surface runoff
297 unaffected by any upstream reservoir operations., i.e., the generated surface runoff drains directly
298 to the reservoir, without passing through any other reservoir. This surface runoff is generated in
299 the part of the watershed which is not shared by any other upstream dams. For instance, in Figure
300 3, the orange and red shaded regions of the watershed will generate the NR for reservoirs B and A
301 respectively. The NR for a reservoir can be estimated using the theoretical inflow into a reservoir
302 if there were no upstream dams, which is referred to as the Theoretical Natural Runoff (TNR) in
303 this paper. The Theoretical Natural Runoff (TNR) refers to the inflow to a reservoir if none of the
304 upstream dams existed. The TNR can be calculated using the following equation –

$$TNR_i = NR_i + \sum_j^N NR_j \quad (3)$$

305 Where, TNR_i is the Theoretical Natural Runoff of reservoir i ; NR_i is the Natural Runoff
306 to reservoir i ; and N is the total number of upstream dams of reservoir i along the same river
307 network. For example, in the schematic in Figure 3, the TNR of reservoir A and B would be NR_A
308 and $NR_B + NR_A$ respectively.

309 Since the TNR represents streamflow into a reservoir in pristine conditions (without
310 considering upstream reservoirs), it is analogous to the modeled inflow at reservoirs using
311 traditional hydrologic models which do not take reservoir operations into account. The NR of any
312 reservoir can be obtained by rearranging the terms of (3), and calculating the NR for reservoirs by
313 iteratively moving downstream for each time-step. The NR for any reservoir can hence be obtained
314 using the TNR of the reservoir, and the NR of the upstream reservoirs using the following equation
315 –

$$NR_i = TNR_i - \sum_j^N NR_j \quad (4)$$

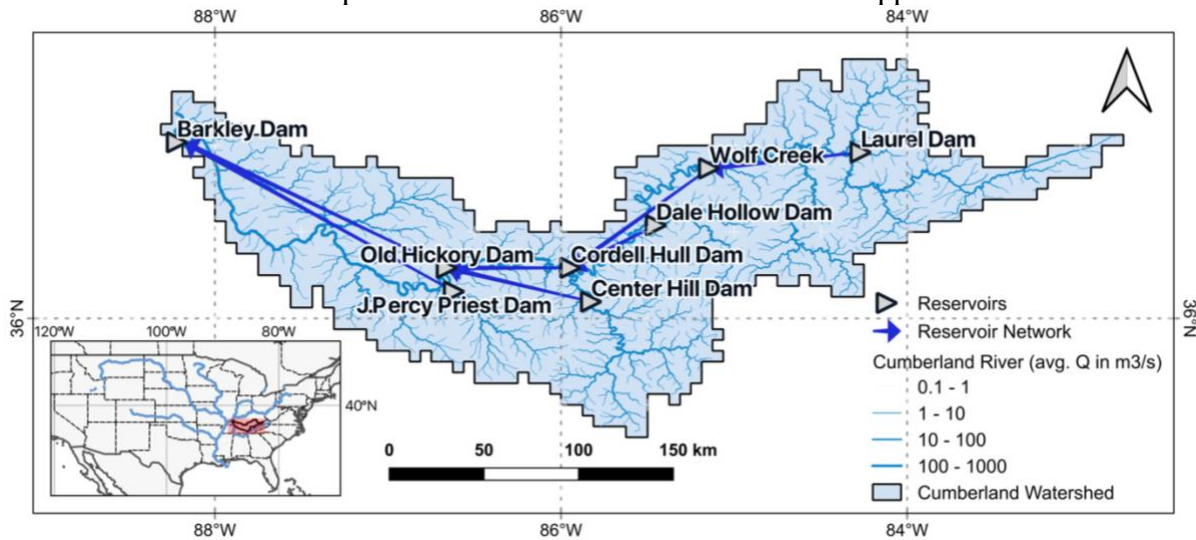
316 Using the estimated NR and RR components, the inflow to a reservoir under regulated
317 conditions is then calculated using (1). Using the storage change of the reservoir, obtained either
318 in-situ or using satellite estimates, the outflow can then be calculated using the water balance
319 equation –

$$O = I - \Delta S \quad (5)$$

320 Where O , I and ΔS are the outflow, inflow and storage change of a reservoir respectively.
321 In the current form of the mass balance equation of the reservoir fluxes, the evaporative losses are
322 not considered. For semi-arid to arid parts of the world, such as the Western US, the Middle East,
323 and Australia, evaporation from reservoirs can play an important role in reservoir water balance
324 (Zhao et al. 2022). For the application ResORR over the Cumberland basin, which has a humid
325 subtropical climate and is a relatively wet region. Here, the evaporative losses from reservoirs do
326 not play a major role in the water balance and was hence safely ignored. For instance, the
327 evaporation from the Wolf Creek reservoir is about only 1-2% of the total inflow to the reservoir
328 annually.

329

These equations were solved for the reservoirs mapped in



330

331 Figure 2 by traversing down the network of reservoirs for each time-step. Since the TNR
 332 is obtained by routing water through the watershed, the travel time of water between the reservoirs
 333 is inherently considered in the subsequent calculations that depend on this routed hydrograph. The
 334 proposed methodology is not a routing scheme, rather it operates on precomputed hydrographs
 335 obtained by routing water through a watershed using traditional routing algorithms. The proposed
 336 algorithm uses observational reservoir operations, either from in-situ or satellite platforms to adjust
 337 the streamflow for regulation due to upstream reservoir operations in a post-processing fashion.

338 To assess the performance of the model, sensitivity to uncertainties in the model inputs,
 339 and generally investigate the limitations of the model, various experiments were setup which are
 340 discussed in section 4.1. To test the theoretical robustness of the proposed river regulation
 341 algorithm as a mass conserving scheme, we set up a two inter-connected linear reservoir problem
 342 where outflow is proportional to water storage and according to the elevation head available at the
 343 outlet. Using this set up we generated regulated inflow that should theoretically happen at the
 344 second reservoir (reservoir 2) based on storage and regulation effect of the upstream reservoir
 345 (reservoir 1). Consequently, we tested the algorithm's ability to mimic the same regulated inflow
 346 to reservoir 2 using storage and upstream unregulated inflow of reservoir 1 that would be available
 347 in a globally scalable manner from satellite observations and modeling platforms such as RAT 3.0.
 348 Our algorithm demonstrated perfect theoretical consistency as a mass conserving scheme. More
 349 details on this theoretical robustness check of the ResORR algorithm are provided in the appendix
 350 (section 7).

351 3.2. Reservoir network

352 The reservoir network represents the connectivity of the reservoirs in the model and is
 353 represented by a directed tree data structure, with the nodes representing the reservoirs and the
 354 links depicting their connectivity, while preserving the order of reservoirs. The model first
 355 topologically sorts the reservoir network, to order them such that the water balance computations
 356 of upstream reservoirs are performed before the subsequent downstream reservoir. At each time-
 357 step, the model iterates over the topologically sorted reservoir network, and solves the series of
 358 equations discussed in 3.1.

359 The reservoir network is generated using the location of reservoirs and the Global
 360 Dominant River Tracing (DRT) dataset (Wu et al., 2011). Since the river-regulation model is
 361 designed as an add-on to the RAT framework, the script to generate the reservoir network can use
 362 the inputs and intermediary outputs of RAT to generate the reservoir network.

363 4. Experiments and Results

364 4.1. River regulation experiment setups using in-situ data

365 The ResORR algorithm is fully described by equations (1)-(5), which uses estimates of
 366 streamflow under pristine conditions from a hydrological model. However, the uncertainties in the
 367 estimations of hydrological model may propagate as uncertainty in the river-regulation model.
 368 Experiments were performed to isolate the performance of the core of the algorithm, its ability to
 369 partition the inflow between the natural and regulated components using in-situ observations in
 370 place of hydrological model and satellite estimates. By reducing uncertainties in certain parts of
 371 the algorithm, the performance of the individual components could be investigated, shedding light
 372 on the sensitivity of the algorithm components to the input data accuracy. Moreover, the observed
 373 in-situ ΔS was used in these experiments to gauge the baseline performance of ResORR using best
 374 available reservoir operations data, avoiding the higher uncertainties normally associated with
 375 satellite estimates of storage change.

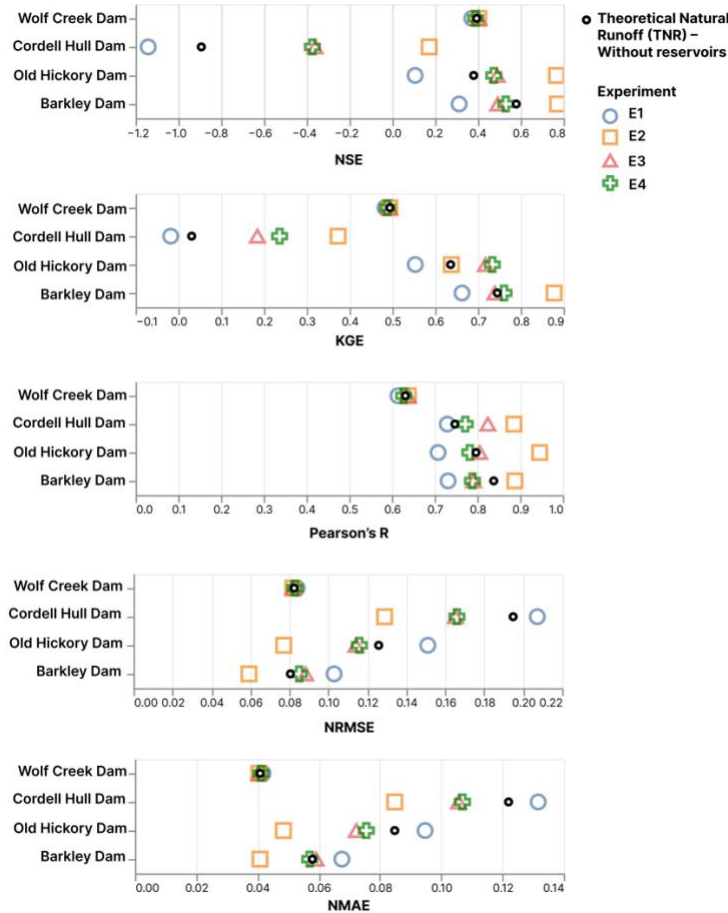
376 To investigate the strengths and weaknesses of ResORR, especially in terms of scalability,
 377 the experiment designs were iteratively modified and updated in order from E1 to E4 over the
 378 period of 2015-2019. Details about the experiment designs and the rationale behind the
 379 experiments are summarized in Table 1.

380 Table 1: Summary of the experiments performed on the river regulation model along with the
 381 corresponding symbols used in the performance comparison plot (Figure 4).

Exp.	In-situ data used	Description	Rationale
E1 	ΔS	In-situ ΔS was used in eqn. (5) to estimate O. VIC hydrologic model was not calibrated for estimating natural inflow.	Uncertainties in satellite estimates of ΔS are minimized in this experiment.
E2 	O	Observed O was used in eqn. (3) to estimate RR.	Uncertainties in otherwise estimated O, due to uncertainties in modeled I are minimized. The RR obtained as such would reflect the “theoretically” best estimate of incoming regulated streamflow.
E3 	I, ΔS	Observed I was used in eqn. (4) only at the most upstream dam, where $NR = TNR = I$. In-situ ΔS was used in (5) to estimate O.	For upstream-most reservoirs all the incoming streamflow would be due to natural runoff, hence, by using the observed I, the uncertainties due to modeled I are minimized. The RR in this

			case would reflect the “theoretical best estimate” of the downstream regulated streamflow.
E4 	ΔS	In-situ ΔS resampled to a 16-day frequency was used in eq (5) to estimate O. The VIC hydrological model, forced with satellite data, was calibrated at upstream most dams of Center Hill Dam, Dale Hollow Dam, and Laurel Dam.	The modeled inflow to the upstream most dams were calibrated using the observed inflow, essentially, minimizing the uncertainties at the upstream boundary of the reservoir network. This represents the ResORR in its globally scalable form under the scenario of perfect ΔS . The resampling to 16-day frequency was done to simulate the observational frequency of the satellite used later in this study.

382 The regulated inflows obtained at the 4 dams, which have at least one upstream dam were
383 compared against the observed inflow at those same dams. The comparison statistics measuring
384 the performance of the river regulation model against observed inflow data are summarized in
385 Figure 4. To understand how the river regulation algorithm is performing under various input
386 scenarios and assumptions, one should compare the relative position of the symbols for each dam
387 along the horizontal axis only. The TNR, obtained from the VIC hydrological model are denoted
388 using grey and black circles, corresponding to the streamflow modeled using default parameter
389 values and calibrated parameters. Formulation of performance metrics are provided in Appendix
390 (section 7).



391
392
393

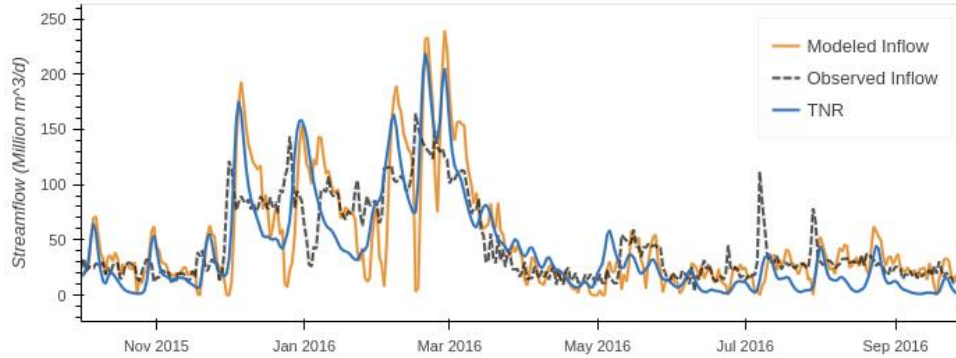
Figure 4: River regulation model performance for E* experiments using in-situ reservoir dynamics data.

394
395
396
397
398
399
400
401
402

Compared to the uncalibrated VIC streamflow estimates, the performance of the river regulation model in the E1 experiment in improving the accuracy of regulated inflow seems to be reduced. In other words, ResORR using in-situ ΔS , but with uncalibrated VIC flow at upstream most location does not improve the skill in predicted regulated inflow at downstream dam locations. However, on taking a closer look at the hydrographs comparing modeled inflow, TNR and observed inflow in Figure 5, it is apparent that the variability in the observed inflow, which is regulated inflow, is more closely replicated by the variability in the modeled inflow than the TNR. This likely suggests that even though the overall performance of ResORR gets reduced as a regulated streamflow predictor, the signature of human regulation is still captured well.

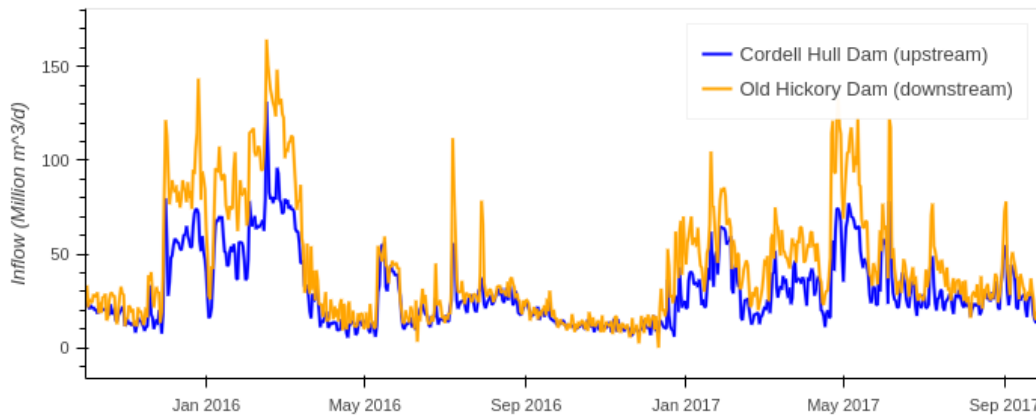
403
404
405
406
407
408
409
410
411

While analyzing the observed inflow hydrographs of two consecutive dams (Cordell Hull and Old Hickory dams) in Figure 6, a closer relationship between the downstream inflow and upstream outflow can be noted. It is clear that the upstream outflow plays a dominant role in dictating the downstream and regulated inflow at the next downstream dam as would be normally expected in the event of no lateral flow diversion. This relationship is further explored in the E2 experiment, where the daily in-situ outflow is used to calculate the RR to the downstream dam. Overall, the results improve across the board in the E2 experiment, underlining the role of upstream reservoir releases in predicting the downstream regulated streamflow. The E2 experiment also stresses the importance of having high accuracy estimates of reservoir storage data.



412
 413 Figure 5: Hydrographs comparing the Modeled, Observed and TNR at Old Hickory Dam, which
 414 is the second most downstream dam in the network. The observed inflow is regulated inflow.

415 In the E3 experiment, the observed inflow to the upstream most dams was used as the NR.
 416 In most cases, the performance of the streamflow predictions still improved when adjusted for
 417 upstream regulation, as compared to the TNR. While this experiment suggests that if the accuracy
 418 of inflow estimates at the upstream most boundary conditions are accurate, that can improve the
 419 regulated streamflow estimates along that downstream network as well. Following this, the final
 420 E4 experiment, representative of the performance of the proposed and scalable river regulation
 421 model under accurate ΔS was performed. Here the VIC hydrological model was calibrated using
 422 the observed inflow at the upstream most dams. The result of this experiment shows overall
 423 improvement for nearly all the reservoirs. These results indicate that using in-situ reservoir
 424 dynamics, specifically storage change, and inflow hydrograph modeled without considering
 425 reservoirs (TNR) can be used to improve the performance of downstream streamflow estimates.



426
 427 Figure 6: Observed inflows at two consecutive dams. The upstream Cordell Hull Dam drains into
 428 the downstream Old Hickory Dam, with the effect of upstream reservoir dynamics.

429 Moreover, the experiment results also shed light on the relationship between the model
 430 performance and the number of upstream dams. For instance, taking the case of the Wolf Creek
 431 dam (7.4 km^3 storage capacity), which only has one upstream dam (Laurel Dam, 0.5 km^3 storage
 432 capacity), the performance of the model does not improve as significantly as compared to the TNR.
 433 On the other hand, Cordell Hull Dam (run-of-the-river) is highly regulated and has two upstream
 434 dams, the Dale Hollow dam (2.1 km^3) and the Wolf Creek dam, and the performance of the
 435 streamflow estimates improves significantly by almost 50% across all the dams in the basin.

436 Overall, the results show that considering the effect of upstream regulation improves the
437 performance of the streamflow estimates at the downstream dams.

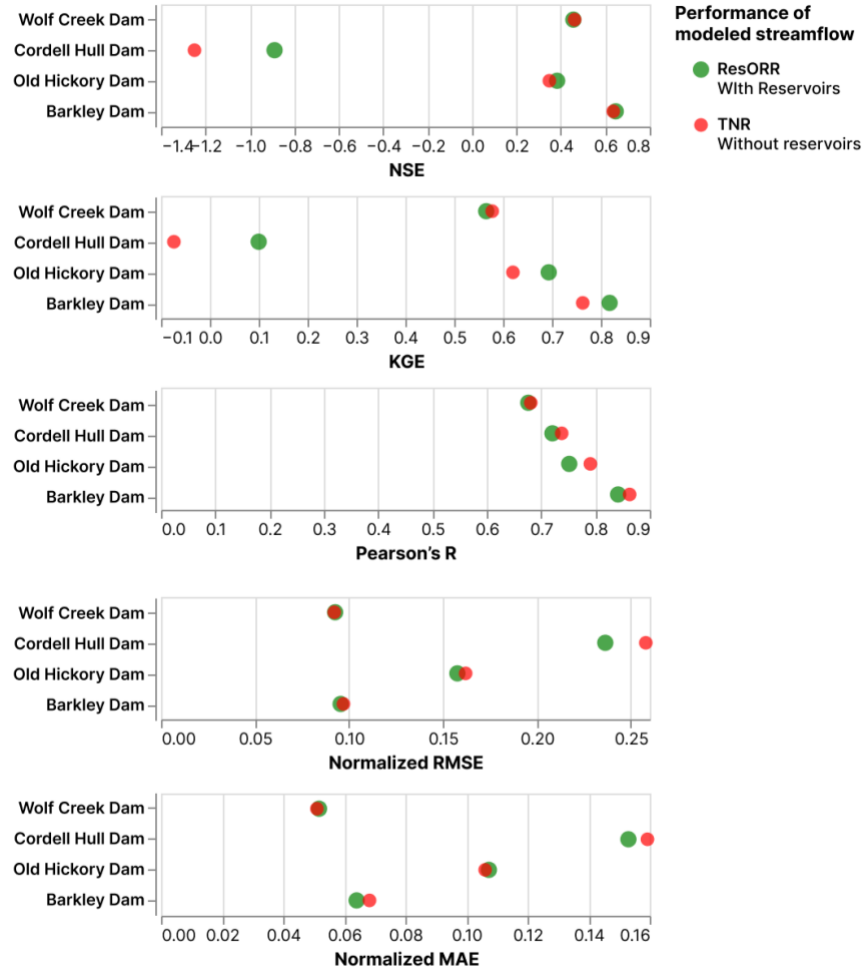
438 4.2. River regulation using satellite estimates of reservoir storage change

439 Now that E4 results established robustness of the proposed river regulation algorithm, we
440 explore how well ResORR fares with satellite-derived ΔS that will have higher uncertainty. The
441 inundation area of the reservoirs were obtained using the Landsat-8 and Sentinel-1 satellite data
442 from June 2018 to October 2019, using the TMS-OS algorithm described by Das et al., (2022).
443 The storage change of the reservoirs were then obtained using these surface area estimates and in-
444 situ Area-Elevation Curve (AEC), using the following equation –

$$445 \quad \Delta S_t = \frac{A_t + A_{t-1}}{2} \times (h_t - h_{t-1}) \quad (6)$$

446 Here the ΔS in equation 6 is the total volumetric storage change, A is the inundation area,
447 and h is the water level height corresponding to the inundation area, obtained using the AEC
448 relationship. The date of satellite observation is denoted by t , with $t - 1$ referring to the last
449 satellite observation. For instance, since Landsat-8 has a revisit period of 16 days, the estimated
450 storage change would refer to the volumetric storage change within those 16 days. These storage
451 change estimates were transformed to daily values by linearly distributing the volumetric change
452 over 16 days. Based on the findings of the previous section, the VIC hydrological model was
453 calibrated at the upstream most dams, like the E4 experiment. The modeled inflow as such and the
454 streamflow estimates from VIC were compared against the observed in-situ inflow. The results are
455 summarized in Figure 7.

456 Similar to the results in the previous section, for the Cordell Hull and Old Hickory, both
457 run-of-the-river dams having upstream dams with large storage capacities, ResORR performance
458 increases significantly across all metrics. For the Wolf Creek dam, adjusting for the upstream
459 Laurel Dam's operations, ResORR performance does not increase as drastically, which can be
460 explained due to the relatively smaller size of the upstream Laurel Dam. In contrast, the
461 performance increases the most for the Cordell Hull Dam, which is preceded by two large dams,
462 Wolf Creek Dam and Dale Hollow dam. The improvement in performance gradually reduces
463 downstream with marginal improvement for the downstream most Barkley Dam. This can be
464 explained by the run-of-the-river nature of the upstream dams, the storage change dynamics of
465 which can be difficult to quantify using satellite observations. Overall, the results suggest that river
466 regulation due to dams can be characterized by the proposed ResORR algorithm using satellite
467 estimates of reservoir storage dynamics. Adjusting for flow regulation due to upstream reservoir
468 storage change improves the overall inflow predictions in a regulated basin.



469
470

Figure 7: ResORR model performance using satellite derived reservoir storage change.

471 **5. Conclusions and Discussion**

472 Rivers of the 21st century are marked with numerous reservoirs, which store, and release
 473 water based on their primary objectives, playing a vital role in providing food, water, and energy
 474 security. However, such reservoir operations can alter the natural streamflow patterns, reducing
 475 the water availability downstream by storing water during high flows, and *vice versa*. In this study,
 476 we developed and tested a scalable river regulation model, ResORR, to predict the regulation of
 477 streamflow due to upstream reservoir operations. Overall, we find that adjusting for upstream
 478 reservoir operations via storage change improves the accuracy of downstream streamflow
 479 predictions. The theoretical basis of the ResORR model was tested using in-situ data in the heavily
 480 regulated Cumberland basin. The results stress the importance of having high accuracy estimates
 481 of both the storage change and the hydrological model. Moreover, we find that if the hydrological
 482 model can be calibrated for boundary conditions of the reservoir network, *i.e.*, at the upstream
 483 most dams, significant improvement can be achieved in predicting regulated inflow at all the
 484 downstream dam locations.

485 Currently, the reservoir network is automatically generated using the dam locations and the
 486 DRT flow directions, and hence, any inter- or intra-basin diversions between reservoirs or lateral

487 diversions cannot yet be modeled. The regulation caused by reservoirs is also determined by its
488 storage capacity, and in a case where a small reservoir drains into a larger reservoir, the algorithm
489 adds little value to the streamflow predictions. Moreover, if the storage change of the upstream
490 reservoir is relatively low, the performance improvement of regulated streamflow estimation
491 downstream can be limited. Such a case was experienced in a case-study of the devastating flood
492 due to extreme precipitation in the state of Kerala, India, in 2018. Due to high precipitation leading
493 up to the main extreme precipitation event, the reservoirs were already at full supply level. All the
494 incoming inflow due to the extreme precipitation event had to be released by the upstream
495 reservoir, with little to no storage change. Even with these limitations, the ResORR algorithm can
496 play an important role in quantifying the regulation of river flow due to reservoirs in changing the
497 world's river systems.

498 With advancements in satellite observations-based reservoir dynamics tracking, especially
499 the RAT 3.0, which has democratized access to reservoir operations information, it is now possible
500 to easily track the operations of reservoirs globally. Building on top of the RAT framework, the
501 proposed river regulation algorithm ResORR would also be able to characterize the regulation of
502 river flow using only satellite-tracked reservoir states at the global scale. The algorithm was
503 developed over the Cumberland basin which is in a humid region. The evaporative losses from the
504 reservoirs therefore play a relatively minor role compared to the inflow into the reservoir due to
505 surface runoff. Hence, the evaporative losses were not considered while calculating the outflow.
506 However, the evaporative losses play an important role in arid region. For application over such
507 regions, the evaporation from the reservoirs can be included in the water mass balance of the
508 reservoirs in eq. (5). The ResORR software architecture is also designed to work seamlessly within
509 the RAT framework, i.e., it can run entirely using the RAT model outputs and intermediary files.
510 With this river regulation tool, the RAT framework will be able to not only infer reservoir
511 dynamics, but also quantify the regulation of streamflow caused by the upstream reservoir
512 operations. We can expect ResORR to soon become a truly scalable algorithm based on the
513 globally available reservoir storage change data of unprecedented accuracy from the Surface Water
514 and Ocean Topography mission.

515 **Acknowledgements:** This study was supported by NASA Applied Science grants from the Water
516 Resources Program (80NSSC22K0918) and the Capacity Building Program (80NSSC23K0184).
517 All co-authors from the University of Washington, co-author Lee from University of Houston, and
518 co-author Andreadis from University of Massachusetts were supported by both these programs.
519

520 **Author role:**

521 Research implementation: Pritam Das

522 Research design, data, and manuscript writing: Pritam Das and Faisal Hossain

523 Data, software and manuscript editing: Sanchit Minocha, George Darkwah and Sarath Suresh

524 Data and manuscript editing: Hyongki Lee and Konstantinos Andreadis

525 Research design and manuscript editing: Miguel Laverde-Barajas and Perry Oddo

526 6. References

- 527 Ahmad, S. K., Hossain, F., Holtgrieve, G. W., Pavelsky, T., & Galelli, S. (2021). Predicting the
528 Likely Thermal Impact of Current and Future Dams Around the World. *Earth's Future*,
529 9(10), e2020EF001916. <https://doi.org/10.1029/2020EF001916>
- 530 Alcamo, J., Döll, P., Henrichs, T., Kaspar, F., Lehner, B., Rösch, T., & Siebert, S. (2003).
531 Development and testing of the WaterGAP 2 global model of water use and availability.
532 *Hydrological Sciences Journal*, 48(3), 317–337.
533 <https://doi.org/10.1623/hysj.48.3.317.45290>
- 534 Biancamaria, S., Lettenmaier, D. P., & Pavelsky, T. M. (2016). The SWOT Mission and Its
535 Capabilities for Land Hydrology. *Surveys in Geophysics*, 37(2), 307–337.
536 <https://doi.org/10.1007/s10712-015-9346-y>
- 537 Biemans, H., Haddeland, I., Kabat, P., Ludwig, F., Hutjes, R. W. A., Heinke, J., von Bloh, W., &
538 Gerten, D. (2011). Impact of reservoirs on river discharge and irrigation water supply
539 during the 20th century. *Water Resources Research*, 47(3).
540 <https://doi.org/10.1029/2009WR008929>
- 541 Biswas, N. K., & Hossain, F. (2022). A Multidecadal Analysis of Reservoir Storage Change in
542 Developing Regions. *Journal of Hydrometeorology*, 23(1), 71–85.
543 <https://doi.org/10.1175/JHM-D-21-0053.1>
- 544 Biswas, N. K., Hossain, F., Bonnema, M., Lee, H., & Chishtie, F. (2021). Towards a global
545 Reservoir Assessment Tool for predicting hydrologic impacts and operating patterns of
546 existing and planned reservoirs. *Environmental Modelling & Software*, 140, 105043.
547 <https://doi.org/10.1016/j.envsoft.2021.105043>

548 Bonnema, M., & Hossain, F. (2017). Inferring reservoir operating patterns across the Mekong
549 Basin using only space observations. *Water Resources Research*, 53(5), 3791–3810.
550 <https://doi.org/10.1002/2016WR019978>

551 Bonnet, M., Witt, A., Steart, K., Hadjerioua, B., & Mobley, M. (2015). *The Economic Benefits of*
552 *Multipurpose Reservoirs in the United States-Federal Hydropower Fleet*.
553 <https://doi.org/10.13140/RG.2.2.15894.14400>

554 Caissie, D. (2006). The thermal regime of rivers: A review. *Freshwater Biology*, 51(8), 1389–
555 1406. <https://doi.org/10.1111/j.1365-2427.2006.01597.x>

556 Cheng, Y., Nijssen, B., Holtgrieve, G. W., & Olden, J. D. (2022). Modeling the freshwater
557 ecological response to changes in flow and thermal regimes influenced by reservoir
558 dynamics. *Journal of Hydrology*, 608, 127591.
559 <https://doi.org/10.1016/j.jhydrol.2022.127591>

560 Cheng, Y., Voisin, N., Yearsley, J. R., & Nijssen, B. (2020). Reservoirs Modify River Thermal
561 Regime Sensitivity to Climate Change: A Case Study in the Southeastern United States.
562 *Water Resources Research*, 56(6), e2019WR025784.
563 <https://doi.org/10.1029/2019WR025784>

564 Cooley, S. W., Ryan, J. C., & Smith, L. C. (2021). Human alteration of global surface water
565 storage variability. *Nature*, 591(7848), Article 7848. [https://doi.org/10.1038/s41586-](https://doi.org/10.1038/s41586-021-03262-3)
566 [021-03262-3](https://doi.org/10.1038/s41586-021-03262-3)

567 Das, P., Hossain, F., Khan, S., Biswas, N. K., Lee, H., Piman, T., Meechaiya, C., Ghimire, U., &
568 Hosen, K. (2022). Reservoir Assessment Tool 2.0: Stakeholder driven improvements to

569 satellite remote sensing based reservoir monitoring. *Environmental Modelling &*
570 *Software*, 157(105533). <https://doi.org/10.1016/j.envsoft.2022.105533>

571 Dong, N., Yang, M., Wei, J., Arnault, J., Laux, P., Xu, S., Wang, H., Yu, Z., & Kunstmann, H. (2023).
572 Toward Improved Parameterizations of Reservoir Operation in Ungauged Basins: A
573 Synergistic Framework Coupling Satellite Remote Sensing, Hydrologic Modeling, and
574 Conceptual Operation Schemes. *Water Resources Research*, 59(3), e2022WR033026.
575 <https://doi.org/10.1029/2022WR033026>

576 Dunn, F. E., Darby, S. E., Nicholls, R. J., Cohen, S., Zarfl, C., & Fekete, B. M. (2019). Projections of
577 declining fluvial sediment delivery to major deltas worldwide in response to climate
578 change and anthropogenic stress. *Environmental Research Letters*, 14(8), 084034.
579 <https://doi.org/10.1088/1748-9326/ab304e>

580 Earth Resources Observation And Science (EROS) Center. (2017). *Shuttle Radar Topography*
581 *Mission (SRTM) 1 Arc-Second Global* [Tiff]. U.S. Geological Survey.
582 <https://doi.org/10.5066/F7PR7TFT>

583 Eldardiry, H., & Hossain, F. (2021). A blueprint for adapting high Aswan dam operation in Egypt
584 to challenges of filling and operation of the Grand Ethiopian Renaissance dam. *Journal*
585 *of Hydrology*, 598, 125708. <https://doi.org/10.1016/j.jhydrol.2020.125708>

586 Gao, H., Birkett, C., & Lettenmaier, D. P. (2012). Global monitoring of large reservoir storage
587 from satellite remote sensing. *Water Resources Research*, 48(9), 2012WR012063.
588 <https://doi.org/10.1029/2012WR012063>

589 Gupta, H. V., Kling, H., Yilmaz, K. K., & Martinez, G. F. (2009). Decomposition of the mean
590 squared error and NSE performance criteria: Implications for improving hydrological

591 modelling. *Journal of Hydrology*, 377(1–2), 80–91.
592 <https://doi.org/10.1016/j.jhydrol.2009.08.003>

593 Haddeland, I., Skaugen, T., & Lettenmaier, D. P. (2006). Anthropogenic impacts on continental
594 surface water fluxes. *Geophysical Research Letters*, 33(8), L08406.
595 <https://doi.org/10.1029/2006GL026047>

596 Han, Z., Long, D., Huang, Q., Li, X., Zhao, F., & Wang, J. (2020). Improving Reservoir Outflow
597 Estimation for Ungauged Basins Using Satellite Observations and a Hydrological Model.
598 *Water Resources Research*, 56(9), e2020WR027590.
599 <https://doi.org/10.1029/2020WR027590>

600 Hanasaki, N., Kanae, S., & Oki, T. (2006). A reservoir operation scheme for global river routing
601 models. *Journal of Hydrology*, 327(1–2), 22–41.
602 <https://doi.org/10.1016/j.jhydrol.2005.11.011>

603 Hanasaki, N., Yoshikawa, S., Pokhrel, Y., & Kanae, S. (2018). A global hydrological simulation to
604 specify the sources of water used by humans. *Hydrology and Earth System Sciences*,
605 22(1), 789–817. <https://doi.org/10.5194/hess-22-789-2018>

606 Hersbach, H., Bell, B., Berrisford, P., Hirahara, S., Horányi, A., Muñoz-Sabater, J., Nicolas, J.,
607 Peubey, C., Radu, R., Schepers, D., Simmons, A., Soci, C., Abdalla, S., Abellan, X.,
608 Balsamo, G., Bechtold, P., Biavati, G., Bidlot, J., Bonavita, M., ... Thépaut, J. (2020). The
609 ERA5 global reanalysis. *Quarterly Journal of the Royal Meteorological Society*, 146(730),
610 1999–2049. <https://doi.org/10.1002/qj.3803>

611 Hossain, F., Sikder, S., Biswas, N., Bonnema, M., Lee, H., Luong, N. D., Hiep, N. H., Du Duong, B.,
612 & Long, D. (2017). Predicting Water Availability of the Regulated Mekong River Basin

613 Using Satellite Observations and a Physical Model. *Asian Journal of Water, Environment*
614 *and Pollution*, 14(3), 39–48. <https://doi.org/10.3233/AJW-170024>

615 Knobon, W. J. M., Freer, J. E., & Woods, R. A. (2019). *Technical note: Inherent benchmark or*
616 *not? Comparing Nash-Sutcliffe and Kling-Gupta efficiency scores* [Preprint]. Catchment
617 hydrology/Modelling approaches. <https://doi.org/10.5194/hess-2019-327>

618 Lee, H., Durand, M., Jung, H. C., Alsdorf, D., Shum, C. K., & Sheng, Y. (2010). Characterization of
619 surface water storage changes in Arctic lakes using simulated SWOT measurements.
620 *International Journal of Remote Sensing*, 31(14), 3931–3953.
621 <https://doi.org/10.1080/01431161.2010.483494>

622 Li, S., Xu, Y. J., & Ni, M. (2021). Changes in sediment, nutrients and major ions in the world
623 largest reservoir: Effects of damming and reservoir operation. *Journal of Cleaner*
624 *Production*, 318, 128601. <https://doi.org/10.1016/j.jclepro.2021.128601>

625 Liang, X., Lettenmaier, D. P., Wood, E. F., & Burges, S. J. (1994). A simple hydrologically based
626 model of land surface water and energy fluxes for general circulation models. *Journal of*
627 *Geophysical Research: Atmospheres*, 99(D7), 14415–14428.
628 <https://doi.org/10.1029/94JD00483>

629 Lohmann, D., Raschke, E., Nijssen, B., & Lettenmaier, D. P. (1998). Regional scale hydrology: I.
630 Formulation of the VIC-2L model coupled to a routing model. *Hydrological Sciences*
631 *Journal*, 43(1), 131–141. <https://doi.org/10.1080/02626669809492107>

632 Marcaida, M., Farhat, Y., Muth, E.-N., Cheythyrit, C., Hok, L., Holtgrieve, G., Hossain, F.,
633 Neumann, R., & Kim, S.-H. (2021). A spatio-temporal analysis of rice production in Tonle

634 Sap floodplains in response to changing hydrology and climate. *Agricultural Water*
635 *Management*, 258, 107183. <https://doi.org/10.1016/j.agwat.2021.107183>

636 Minocha, S., Hossain, F., Das, P., Suresh, S., Khan, S., Darkwah, G., Lee, H., Galelli, S., Andreadis,
637 K., & Oddo, P. (2023). Reservoir Assessment Tool Version 3.0: A Scalable and User-
638 Friendly Software Platform to Mobilize the Global Water Management Community.
639 *Geoscientific Model Development Discussions*, 2023, 1–23.
640 <https://doi.org/10.5194/gmd-2023-130>

641 Nash, J. E., & Sutcliffe, J. V. (1970). River flow forecasting through conceptual models part I — A
642 discussion of principles. *Journal of Hydrology*, 10(3), 282–290.
643 [https://doi.org/10.1016/0022-1694\(70\)90255-6](https://doi.org/10.1016/0022-1694(70)90255-6)

644 Neel, J. K., & Allen, W. R. (1964). The mussel fauna of the upper Cumberland Basin before its
645 impoundment. *Malacologia*, 1(3), 427–459.

646 Okeowo, M. A., Lee, H., Hossain, F., & Getirana, A. (2017). Automated Generation of Lakes and
647 Reservoirs Water Elevation Changes From Satellite Radar Altimetry. *IEEE Journal of*
648 *Selected Topics in Applied Earth Observations and Remote Sensing*, 10(8), 3465–3481.
649 <https://doi.org/10.1109/JSTARS.2017.2684081>

650 Pokhrel, Y., Shin, S., Lin, Z., Yamazaki, D., & Qi, J. (2018). Potential Disruption of Flood Dynamics
651 in the Lower Mekong River Basin Due to Upstream Flow Regulation. *Scientific Reports*,
652 8(1), Article 1. <https://doi.org/10.1038/s41598-018-35823-4>

653 Robinson, J. A. (2019). *Estimated use of water in the Cumberland River watershed in 2010 and*
654 *projections of public-supply water use to 2040* (Report 2018–5130; Scientific

655 Investigations Report, p. 74). USGS Publications Warehouse.
656 <https://doi.org/10.3133/sir20185130>

657 Steyaert, J. C., Condon, L. E., W. D. Turner, S., & Voisin, N. (2022). ResOpsUS, a dataset of
658 historical reservoir operations in the contiguous United States. *Scientific Data*, 9(1),
659 Article 1. <https://doi.org/10.1038/s41597-022-01134-7>

660 Suresh, S., Hossain, F., Minocha, S., Das, P., Khan, S., Lee, H., Andreadis, K., & Oddo, P. (2024).
661 Satellite-based Tracking of Reservoir Operations for Flood Management during the 2018
662 Extreme Weather Event in Kerala, India. *Remote Sensing of Environment*, 1–34.

663 Tippit, R. N., Brown, J. K., Sharber, J. F., & Miller, A. C. (1995). Modifying Cumberland River
664 system reservoir operations to improve mussel habitat. *Conservation and Management*
665 *of Freshwater Mussels II: Initiatives for the Future. Proceedings of a UMRCC Symposium*,
666 229–235.

667 USACE. (n.d.). *WM Data Dissemination*. Retrieved October 15, 2023, from
668 <https://water.usace.army.mil/a2w/f?p=100:1:.....#>

669 Vanderkelen, I., Gharari, S., Mizukami, N., Clark, M. P., Lawrence, D. M., Swenson, S., Pokhrel,
670 Y., Hanasaki, N., van Griensven, A., & Thiery, W. (2022). Evaluating a reservoir
671 parametrization in the vector-based global routing model mizuRoute (v2.0.1) for Earth
672 system model coupling. *Geoscientific Model Development*, 15(10), 4163–4192.
673 <https://doi.org/10.5194/gmd-15-4163-2022>

674 Vu, D. T., Dang, T. D., Galelli, S., & Hossain, F. (2021). *Satellite observations reveal thirteen years*
675 *of reservoir filling strategies, operating rules, and hydrological alterations in the Upper*
676 *Mekong River Basin* [Preprint]. Hydrology. <https://doi.org/10.1002/essoar.10507302.1>

677 Wada, Y., Bierkens, M. F. P., de Roo, A., Dirmeyer, P. A., Famiglietti, J. S., Hanasaki, N., Konar,
678 M., Liu, J., Müller Schmied, H., Oki, T., Pokhrel, Y., Sivapalan, M., Troy, T. J., van Dijk, A. I.
679 J. M., van Emmerik, T., Van Huijgevoort, M. H. J., Van Lanen, H. A. J., Vörösmarty, C. J.,
680 Wanders, N., & Wheeler, H. (2017). Human–water interface in hydrological modelling:
681 Current status and future directions. *Hydrology and Earth System Sciences*, 21(8), 4169–
682 4193. <https://doi.org/10.5194/hess-21-4169-2017>

683 Wilson, C. B., & Clark, H. W. (1914). *The mussels of the Cumberland River and its tributaries*
684 (Issue 781). US Government Printing Office.

685 Wissler, D., & Fekete, B. M. (2009). *Reconstructing 20th century global hydrography*.

686 Wu, H., Kimball, J. S., Mantua, N., & Stanford, J. (2011). Automated upscaling of river networks
687 for macroscale hydrological modeling: UPSCALING OF GLOBAL RIVER NETWORKS. *Water*
688 *Resources Research*, 47(3). <https://doi.org/10.1029/2009WR008871>

689 Yoon, Y., & Beighley, E. (2015). Simulating streamflow on regulated rivers using characteristic
690 reservoir storage patterns derived from synthetic remote sensing data. *Hydrological*
691 *Processes*, 29(8), 2014–2026. <https://doi.org/10.1002/hyp.10342>

692 Yoon, Y., Beighley, E., Lee, H., Pavelsky, T., & Allen, G. (2016). Estimating Flood Discharges in
693 Reservoir-Regulated River Basins by Integrating Synthetic SWOT Satellite Observations
694 and Hydrologic Modeling. *Journal of Hydrologic Engineering*, 21(4), 05015030.
695 [https://doi.org/10.1061/\(ASCE\)HE.1943-5584.0001320](https://doi.org/10.1061/(ASCE)HE.1943-5584.0001320)

696 Zhao, G., Li, Y., Zhou, L., & Gao, H. (2022). Evaporative water loss of 1.42 million global lakes.
697 *Nature Communications*, 13(1), 3686. <https://doi.org/10.1038/s41467-022-31125-6>

698 Zhou, T., Nijssen, B., Gao, H., & Lettenmaier, D. P. (2016). The Contribution of Reservoirs to
699 Global Land Surface Water Storage Variations. *Journal of Hydrometeorology*, 17(1), 309–
700 325. <https://doi.org/10.1175/JHM-D-15-0002.1>

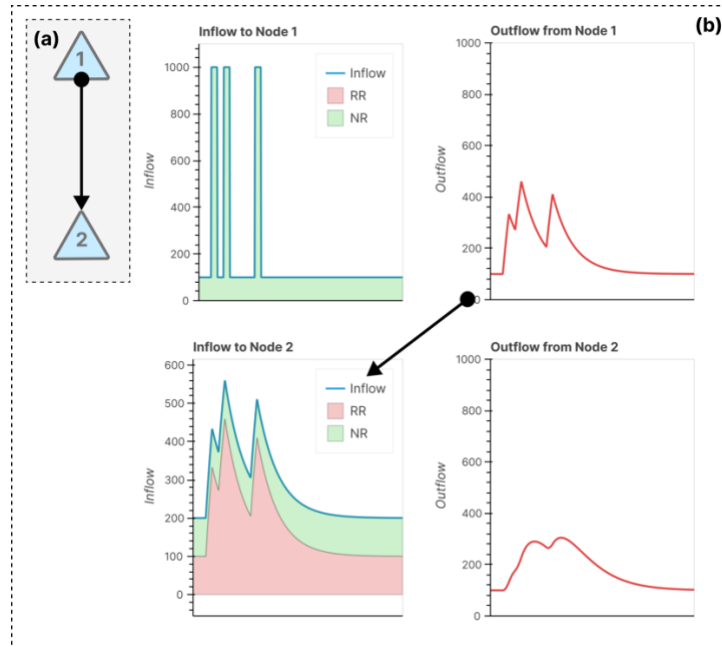
701

702

703 7. Appendix

704 7.1. River-regulation algorithm ResORR tested in a theoretical two- 705 reservoir system using synthetic data

706 A theoretical two inter-connected linear reservoir system with artificially generated
707 headwater flow inputs was used to test the theoretical robustness of the mass conserving and
708 numerical stability of the ResORR algorithm. This classic problem (Figure 8) also helped visualize
709 the outputs of ResORR algorithm and verify if mass balance is maintained.



710 Figure 8: (a) Schematic showing the two-reservoir system setup. The black arrow denotes the
711 direction of flow of water. (b) Hydrographs showing inflow and outflow from nodes 1 and 2. In
712 this case, three input pulses of 1000 L³/T units were fed into node 1, and its outflow was treated
713 as the inflow to the downstream node 2. The inflow and outflow at node 2 represent the
714 ‘theoretical’ answer for the ResORR algorithm to be theoretically valid.
715

716 A system of two interconnected linear reservoirs were set up, like the schematic shown in
717 Figure 8. To understand how the outflow from an upstream reservoir would affect the inflow to
718 the downstream reservoir, we first generated a synthetic headwater inflow hydrograph for reservoir
719 1 and then applied ResORR to predict the regulated inflow to the downstream reservoir at node 2.
720 Both the reservoirs were provided with a constant water influx of 100 L³/T units in the form of
721 natural runoff, NR. Additionally, the upstream reservoir, at node 1, was provided with three pulses
722 of high inflow volumes of 1000 L³/T units. The reservoirs were treated as linear reservoirs, where
723 the outflow from a reservoir at any given time as a linear function of the instantaneous storage,
724 and can be defined as follows –

$$725 \quad O = K \times S$$

726 Where, $K [T^{-1}]$ is the reaction factor, which determines how quickly the reservoir drains
727 ($K = 0.01$ in this experiment). The outflow from the upstream reservoir at node 1 was then treated
728 as the regulated runoff, RR for the downstream reservoir, node 2. Using the inflows and outflows

729 obtained at both the reservoirs, the storage change was obtained using (5). The theoretical natural
 730 runoff, TNR, was also obtained using (3). The ResORR was then run using this simulated storage
 731 change and TNR information as inputs, to model the inflow at both the reservoirs. The modeled
 732 inflow of ResORR was then compared with the synthetically generated inflow at the downstream
 733 node 2, with a perfect match between them. The closure of water balance was also tested by
 734 comparing the total inflow volumes in the modeled and synthetic inflow.

735 7.2. Performance metrics used for assessing ResORR

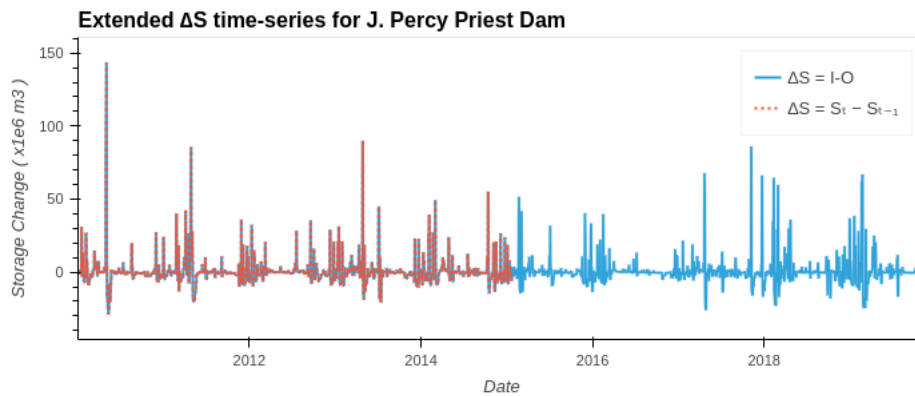
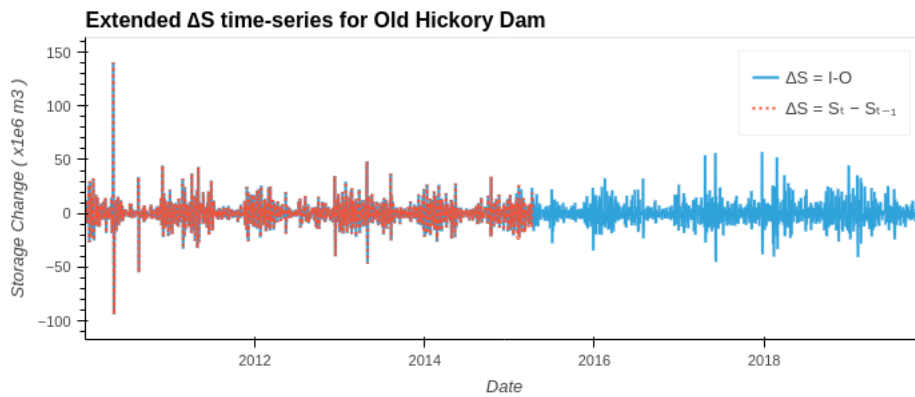
736 The following five commonly used performance metrics were used in this study to quantify
 737 the skill of the river regulation model -

Metric	Equation	Description
Nash-Sutcliffe Efficiency (NSE) (Nash & Sutcliffe, 1970)	$1 - \frac{\sum_{t=1}^T (Q_O^t - Q_M^t)^2}{\sum_{t=1}^T (Q_O^t - \overline{Q_O})^2}$ <p>Where, Q_O^t and Q_M^t are observed and modeled streamflow respectively. $\overline{Q_O}$ is the mean observed streamflow.</p>	The NSE can vary between $-\infty$ and 1. A value of 1 indicates a perfect match between observed and modeled values. A value of 0 indicates that the model predictions are as performant as using the mean of the observed values as a predictor. Higher values are better.
Kling-Gupta Efficiency (KGE) (Gupta et al., 2009)	$1 - \sqrt{(r - 1)^2 + (\alpha - 1)^2 + (\beta - 1)^2}$ <p>Where, r is the linear correlation between modeled and observed values, $\alpha = \left(\frac{\sigma_M}{\sigma_O} - 1\right)^2$, σ_M and σ_O are the standard deviations of the modeled and observed values, $\beta = \left(\frac{\mu_M}{\mu_O} - 1\right)^2$, μ_M and μ_O are mean modeled and observed values.</p>	The KGE varies between $-\infty$ and 1. A value of -0.41 indicates model performance equal to using the mean of the observed values as a predictor (Knoben et al., 2019). Higher values are better.
Pearson's R	$\frac{cov(Q_O, Q_M)}{\sigma_O \sigma_M}$ <p>Where, $cov(Q_O, Q_M)$ is the covariance of the observed and modeled values. σ_M and σ_O are the standard deviations of the modeled and observed values</p>	The Pearson's R can vary from -1 to 1, where 1 indicates a perfect positive linear correlation. A value of 0 indicates no correlation.
Normalized Root-Mean Squared Error (NRMSE)	$\frac{\sqrt{\frac{\sum_{i=1}^N (Q_O - Q_M)^2}{N}}}{\max(Q_O) - \min(Q_O)}$ <p>Where, $\max(Q_O)$ and $\min(Q_O)$ are the maximum and minimum observed streamflow values.</p>	The NRMSE represents the standard deviation of the residuals as a fraction of the range of the observed values. Lower values are better.

<p>Normalized Mean Absolute Error (NMAE)</p>	$\frac{\sum_{i=1}^N Q_M - Q_O }{\max(Q_O) - \min(Q_O)}$ <p>Where, N is the number of observations, $Q_M - Q_O$ is the absolute difference of modeled and observed values</p>	<p>The NMAE represents the average absolute difference between observed and modeled values as a fraction of the range of observed values. Lower values are better.</p>
--	---	--

738 **7.3. Handling missing In-situ storage data**

739 Two dams in the basin, Old Hickory and Laurel, had missing in-situ storage data after April
740 2015, due to which storage change could not be calculated using observed (in-situ) storage. This
741 missing data was filled by assuming water mass-balance owing to inflow and outflow from the
742 reservoirs, $\Delta S = I - O$.



744

745